

**This item is the archived peer-reviewed author-version of:**

Evaluating the role of recycling rate and rejuvenator on the chemo-rheological properties of reclaimed polymer-modified binders

**Reference:**

Margaritis Alexandros, Pipintakos Georgios, Jacobs Geert, Hernando David, Bruynen Mats, Bruurs Jeroen, Van den bergh Wim.- Evaluating the role of recycling rate and rejuvenator on the chemo-rheological properties of reclaimed polymer-modified binders  
Road materials and pavement design : an international journal - ISSN 1468-0629 - 22:s1(2021), p. S83-S98  
Full text (Publisher's DOI): <https://doi.org/10.1080/14680629.2021.1905700>  
To cite this reference: <https://hdl.handle.net/10067/1773990151162165141>

1 **Evaluating the role of recycling rate and rejuvenator on the**  
2 **chemo-rheological properties of reclaimed polymer-modified binders**

3 Alexandros Margaritis<sup>a</sup>, Georgios Pipintakos<sup>a</sup>, Geert Jacobs<sup>a</sup>, David  
4 Hernando<sup>a</sup>, Mats Bruynen<sup>a</sup>, Jeroen Bruurs<sup>a</sup> & Wim Van den bergh<sup>a\*</sup>

5 <sup>a</sup> *Faculty of Applied Engineering, EMIB research group, University of Antwerp,*  
6 *Antwerp, Belgium;*

7 [\\*wim.vandenbergh@uantwerpen.be](mailto:wim.vandenbergh@uantwerpen.be)

8

9

10

11 Alexandros Margaritis: 0000-0003-3639-020X

12 Georgios Pipintakos: 0000-0002-7027-2672

13 Geert Jacobs: 0000-0002-8362-5609

14 David Hernando: 0000-0001-8284-5792

15 Wim Van den bergh: 0000-0002-0897-1392

16

17

18

19

20

21

22

23

24 Word count: 5701

## 25 **Evaluating the role of recycling rate and rejuvenator on the** 26 **chemo-rheological properties of reclaimed polymer-modified binders**

27       Incorporating reclaimed asphalt (RA) is a very common practice, although its use  
28       in premium surface layer mixtures is still limited due to performance concerns.  
29       This task becomes even more challenging when combining aged polymer-  
30       modified bitumen (PMB) with virgin PMB. For this reason, the objective of this  
31       study is to evaluate, from a binder perspective, the feasibility of incorporating  
32       reclaimed polymer-modified binder (RPMB) in new surface layer mixtures. To  
33       address this challenge, blends of RPMB and virgin PMB were investigated at three  
34       replacement rates (20%, 40% and 60%) with and without a tall oil-based  
35       rejuvenator. Changes in viscoelastic behaviour were assessed through several  
36       performance indices obtained from dynamic shear rheometer testing. Moreover,  
37       physicochemical changes were tracked using infrared spectroscopy and  
38       fluorescence microscopy. The experimental investigation revealed that, due to  
39       polymer degradation of the RMPB, only the blends with 20% RMPB exhibited  
40       polymer activity. Finally, the use of the rejuvenator successfully compensated for  
41       the rheological properties of the aged RPMB and reduced the susceptibility to non-  
42       load-associated cracking but did not contribute to polymer activity restoration.

43       Keywords: reclaimed asphalt binder; recycling; polymer-modified binder (PMB);  
44       rejuvenator; polymer activity; rheology;

### 45 **Introduction**

46       In an era where environmental preservation becomes a necessity, the road industry has  
47       taken considerable actions towards more sustainable solutions. Asphalt recycling is a  
48       widely accepted sustainable solution, offering both economic and environmental  
49       benefits (Anthonissen et al., 2016; Aurangzeb et al., 2014). In this context, extensive  
50       research has been conducted to evaluate the performance of asphalt mixtures when  
51       incorporating high rates of reclaimed asphalt (RA), pointing out possible issues in terms  
52       of cracking performance (Zaumanis & Mallick, 2015). The main challenges when  
53       designing a mixture with RA are to restore its aged properties and to achieve the

54 satisfactory performance necessary for its new role in the pavement structure. Among  
55 the compensation actions typically taken are the utilisation of chemical agents such as  
56 rejuvenators and modifiers (Bajaj et al., 2020; Kodippily et al., 2017).

57 To date, RA has been mostly incorporated in base layers and, to a lower extent,  
58 in surface layers. Higher performance requirements for surface layer mixtures have led  
59 to a more conservative approach, although some studies have investigated the use of up  
60 to 40% in dense-graded surface mixtures (Y. Yan et al., 2017; Y. Yan et al., 2019). Still,  
61 recycling in surface layers is limited or banned by road agencies when premium  
62 mixtures, commonly produced with styrene-butadiene-styrene (SBS) polymer-modified  
63 binder (PMB), are used. That is the case of Flanders (Belgium), where their premium  
64 surface layer (stone mastic asphalt) is not allowed to be recycled into new surface layers  
65 in public works. This leads to downcycling premium RA, composed of high-quality  
66 aggregate and aged PMB, into new base layer mixtures.

67 A challenging task that remains is the reuse of reclaimed polymer modified  
68 binder (RPMB), as there is uncertainty in how the aged polymer participates in the new  
69 blend. An earlier study by Liu et al. showed that RPMB combined with virgin PMB  
70 exhibited some polymer-modification characteristics, but it depended on the type of  
71 RPMB and treatment (Liu et al., 2015). Given the fact that surface layer mixtures  
72 commonly use styrene-butadiene-styrene (SBS) triblock copolymer as a modifier  
73 (Yildirim, 2007), a detailed exploration for the potential reuse of this type of RPMB is  
74 still missing.

75 The use of rejuvenators attempts to restore the deterioration of bitumen due to  
76 ageing (Jacobs et al., 2021). What is still missing is a clear understanding of its  
77 interaction with PMB and in particular their effect on SBS degradation. The level of  
78 polymer activity and the effectiveness of the rejuvenating agent can be investigated by

79 assessing various rheological parameters. For example, complex modulus and phase  
80 angle master curves can reflect the temperature susceptibility of the material, especially  
81 for complex binders like PMB (Airey, 2003). Other parameters, like high-temperature  
82 true grade or parameters based on the multiple stress creep-recovery (MSCR) test, can  
83 give an indication on rutting resistance (D'Angelo et al., 2007; Domingos & Faxina,  
84 2016). Furthermore, it has been suggested that the cracking performance of rejuvenated  
85 recycled blends can be evaluated using the Glover-Rowe (G-R) parameter (Garcia  
86 Cucalon et al., 2019; G. M. Rowe & Sharrock, 2016). Moreover, the crossover  
87 frequency ( $\omega_c$ ), which is the point where the viscous and elastic contributions are equal,  
88 has been claimed to relate well to relaxation and consequently, to non-load-associated  
89 cracking (D. W. Christensen et al., 2017).

90 An issue of paramount importance is the compatibility of SBS with the bitumen  
91 (Masson et al., 2003), especially when aged PMB is incorporated in new blends.  
92 Asphalt production and environmental conditions influence the polymer and the  
93 bitumen differently, leading to a degradation of the polymer chains (chain scission) as a  
94 result of ageing (Lu & Isacson, 1998; Yut & Zofka, 2011). A common practice to  
95 analyse bitumen composition is the separation into generic fractions according to their  
96 polarity, ranging from the more polar asphaltenes to the less polar aromatics, resins and  
97 saturates. Researchers have attributed the SBS-degradation phenomenon to the swelling  
98 of polymers by the lighter compounds, typically aromatics (Lesueur, 2009). This  
99 process contributes to an increase in asphaltenes and subsequently, to a more severe  
100 stiffening of the SBS bitumen (Kleiziene et al., 2019).

101 Previous studies have reached a number of conclusions regarding the ageing  
102 mechanisms that evolve in bitumen (Pipintakos et al., 2020). However, the role of  
103 polymer presence is yet to be understood. Fourier-transform infrared spectroscopy

104 (FTIR) offers the possibility to unravel, at least partially, the influence of recycling rate  
105 and the degradation severity of the SBS. For that purpose, standard infrared ageing  
106 indices can account for the functionality of the rejuvenator and the effect in the  
107 polymer-related chemical groups, which are an easy target for oxygen due to the  
108 unsaturated double-carbon bonds of the polybutadiene blocks (C. Yan et al., 2018).

109 Undoubtedly, the assessment of new blends and the role of the polymer in these  
110 blends becomes a complex task, given the fact that various mechanisms take place.

111 Previous efforts have shown that rheological and chemical properties are able to track  
112 polymer activity and degradation as well as the effectiveness of a rejuvenating agent to  
113 restore the ageing properties of PMB-free RA. However, the gap here is that limited  
114 studies have addressed the residual effects of RPMB, namely elasticity after degradation  
115 when incorporated at various rates. Another important aspect missing is whether a  
116 rejuvenator can have an added value into restoring an RPMB.

117 The focus of this paper is to address the effect of adding RPMB in new binder  
118 blends at various replacement rates, and the effect of using a rejuvenator, a typical  
119 practice nowadays when PMB-free RA is considered. Besides assessing the effect of  
120 recycling rate and use of a rejuvenator, another goal was to evaluate which tests are  
121 sensitive to capture changes among the studied blends and more importantly, to capture  
122 whether the old polymer is still active and up to which recycling rate. The motivation of  
123 this research is a first step into investigating the potential of horizontal recycling (SMA  
124 into an SMA) and not downcycling (SMA to an AC base).

## 125 **Objectives**

126 In this study, blends of RPMB and virgin PMB are rheologically and physicochemically  
127 assessed at a binder level. The following objectives were set to address more specific

128 research questions:

- 129 • To investigate the relationship between the recycling rate of reclaimed polymer-  
130 modified binder (RPMB) and the performance of blends with virgin polymer  
131 modified binder (PMB).
- 132 • To explore whether the addition of a bio-based rejuvenator is beneficial to the  
133 chemo-rheological properties of the blends.
- 134 • To assess the level of polymer activity in blends of RPMB and virgin PMB with  
135 and without rejuvenator.

## 136 **Materials and methods**

### 137 *Binder sources*

138 This study uses an RPMB source and a virgin PMB as primary materials. The RPMB is  
139 a modified binder from a single road source, extracted and recovered using  
140 trichloroethylene as a solvent according to EN 12697-1:2012. The original properties of  
141 the RPMB are not known; however, preliminary FTIR analyses identified SBS-related  
142 peaks and thus, the observed peaks can be clearly assigned to SBS presence. The  
143 reference binder is a commercially available PMB (type 40/100-75) modified with SBS.  
144 Therefore, both RPMB and PMB are SBS-based binders.

### 145 *Binder blend design*

146 Three binder replacements rates were considered: 20%, 40% and 60% (percentage by  
147 mass of total binder blend). Additionally, the virgin PMB and the field-aged binder  
148 (100% RPMB) were tested, referred to as REF and 100% RA samples, respectively.  
149 The three replacement rates were also treated with a rejuvenator to investigate its  
150 influence on the chemo-rheological characteristics of the blends. A rejuvenator

151 originating from crude tall oil was selected based on its bio-based origin, commercial  
 152 availability and previous experiences with RPMB. The rejuvenator has a yellow colour  
 153 and is liquid at room temperature, with a flash point above 280°C and kinematic  
 154 viscosity of 100 mm<sup>2</sup>/s at 20°C. Its dosage was determined to achieve a penetration  
 155 value similar to that of the reference binder. To keep the recycling rates with and  
 156 without rejuvenator comparable, the amount of rejuvenator was subtracted from the  
 157 virgin binder quantity. An overview of the composition of the blends is presented in  
 158 Table 1. The binder blends without rejuvenator were labelled as “replacement rate +  
 159 RA” and the blends with rejuvenator as “replacement rate + REJ”.

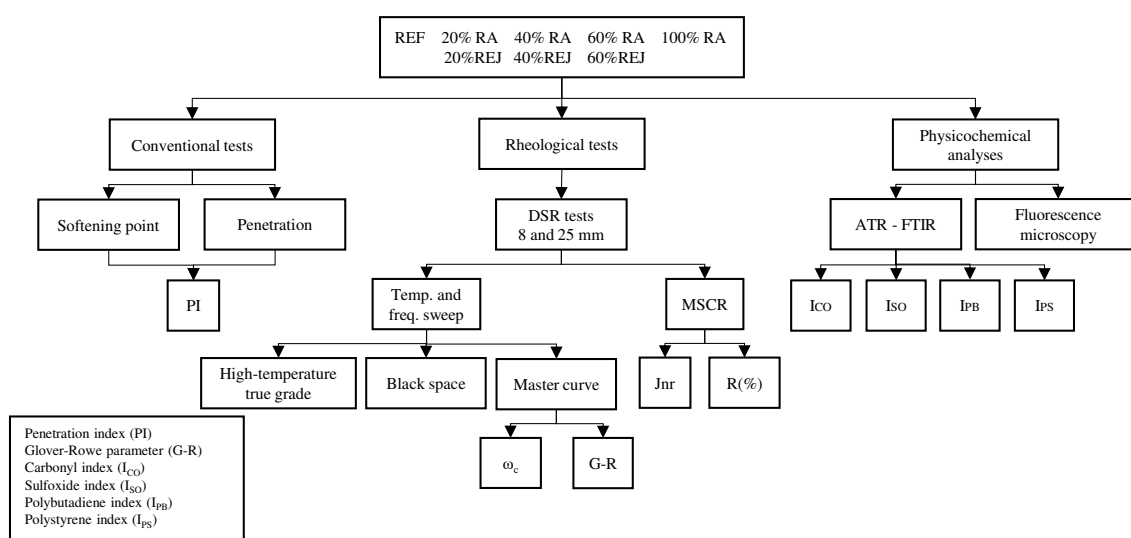
160 Before blending in batches of 65 grams, the constituent binders were placed in  
 161 an oven at 170°C for 30 minutes and then stirred separately for 5 minutes on a heating  
 162 element. The stirring was performed with a low shear mixer and at a speed of  
 163 250 min<sup>-1</sup>. After 15 additional minutes in the oven and 1 minute of stirring, the blends  
 164 were prepared by adding the correct amounts of RPMB, rejuvenator (at room  
 165 temperature) and virgin PMB. The final blends were mixed again for 1 minute after  
 166 another heating period of 5 minutes in the oven.

167 Table 1: Summary of the blends and their composition (percentage by mass of total  
 168 binder)

Name	PMB (%)	RPMB (%)	Rejuvenator (%)
REF	100.0	0.0	0.0
20% REJ	78.2	20.0	1.8
40% REJ	56.4	40.0	3.6
60% REJ	34.3	60.0	5.1
20% RA	80.0	20.0	0.0
40% RA	60.0	40.0	0.0
60% RA	40.0	60.0	0.0
100% RA	0.0	100.0	0.0

169 **Experimental methods**

170 Binder blends were subjected to a suite of tests for performance evaluation. First,  
 171 conventional tests were carried out on each blend. Then, rheological tests were  
 172 conducted to evaluate the viscoelastic behaviour and to define certain performance  
 173 parameters. Finally, physicochemical analyses were performed to assess changes  
 174 derived from the introduction of RPMB and rejuvenator. The concerning tests and  
 175 analyses are summarised in Figure 1 and described in the next sections.



176  
 177 **Figure 1: Flowchart of experimental methods**

178 **Conventional tests**

179 Penetration and softening point values were determined according to EN 1426:2015 and  
 180 EN 1427:2015, respectively. From penetration and softening point values, the  
 181 penetration index (PI) was calculated to obtain an indication of temperature  
 182 susceptibility.

183 **Rheological tests**

184 Rheological properties were assessed using a dynamic shear rheometer (DSR)  
 185 according to EN 14770:2012. Frequency sweeps were performed utilising an Anton

186 Paar™ MCR 500 DSR, equipped with an 8 and 25 mm parallel plate geometry in a  
187 temperature range from 0°C to 100°C, with steps of 10°C. Frequencies from 1 to 10 Hz  
188 were applied in a strain-controlled mode within the linear viscoelastic region of the  
189 binder blends. For every blend, two replicates were tested. The results were processed  
190 using the RHEA™ software (Abatech, 2011), and the master curves were constructed at  
191 a reference temperature of 20°C based on the Christensen-Anderson (CA) model (D. W.  
192 J. Christensen & Anderson, 1992). The crossover frequency ( $\omega_c$ ) used in this model is  
193 considered the frequency where the viscous and elastic contributions are equal. This  
194 parameter is used to evaluate the viscoelastic behaviour of binder blends, and it has also  
195 been proposed as a stress relaxation indicator (Jing et al., 2020).

196 Another commonly used parameter is the Glover-Rowe parameter (G-R), which  
197 indicates the susceptibility to non-load-associated cracking. This parameter was  
198 calculated using equation (1) with  $G^*$  and phase angle ( $\delta$ ) at a temperature of 15°C and  
199 a frequency of 0.005 rad/s (G. Rowe et al., 2014). Previous studies introduced G-R  
200 limits of 180 kPa and 600 kPa to indicate the onset of cracking (warning limit) and  
201 extensive block cracking (critical limit), respectively (D. Christensen et al., 2019).

$$202 \quad G - R = \frac{G^* (\cos \delta)^2}{\sin \delta} \quad (1)$$

203 Since PMB is also utilised to improve the characteristics at high service  
204 temperatures, the MSCR test was performed to assess the binder resistance to  
205 permanent deformation. The MSCR test was performed according to EN 16659:2016 in  
206 the 25 mm geometry of the DSR at 50°C. This temperature was selected since it  
207 corresponds to the rutting test temperature in the Flemish region (Agentschap Wegen en  
208 Verkeer, 2019). The main parameters extracted from this test are the average recovery  
209 percentages ( $R_{100}$  and  $R_{3200}$ ), which indicate the recoverable shear strain, and the non-

210 recoverable creep compliances ( $J_{nr,100}$  and  $J_{nr,3200}$ ), which are the unrecovered shear  
211 strains divided by the applied shear stresses. They are calculated at shear stress levels of  
212 100 Pa and 3200 Pa.

### 213 ***Physicochemical analyses***

214 The attenuated total reflectance Fourier-transform infrared spectroscopy (ATR-FTIR)  
215 analysis method is a technique that uses infrared light to observe changes in chemical  
216 bonds. In this study, the test was performed taking 32 repetitive scans on a binder  
217 sample using a Thermo Fisher Scientific Nicolet iS™ 10 spectrometer. The scans were  
218 performed with a resolution of  $4\text{ cm}^{-1}$  in a range between  $4000\text{ cm}^{-1}$  and  $400\text{ cm}^{-1}$ . The  
219 average of the 32 scans yields a spectrum that is normalised before analysis. The  
220 normalisation procedure is based on the methods described in previous studies (Hofko  
221 et al., 2018; Margaritis et al., 2020): first, the spectra are shifted to an absorbance of 0 at  
222  $1753\text{ cm}^{-1}$ . Then, the spectra are scaled to an absorbance of 1 at  $2923\text{ cm}^{-1}$ .

223 The analysis of the spectra allows the identification of chemical bonds present in  
224 the material. To assess the ageing state of the binders, the carbonyl and sulfoxide areas  
225 are generally considered as effective indicators (Marsac et al., 2014). Also, traces of  
226 modification with SBS can be captured around two distinctive peaks: one at  $966\text{ cm}^{-1}$   
227 (polybutadiene area) and another one at  $699\text{ cm}^{-1}$  (polystyrene area). The calculation of  
228 the indices is performed by dividing the integration of the area over the integration of a  
229 reference area. The areas were integrated using the tangential valley-to-valley approach.  
230 A reference area that is stable during ageing, the aliphatic group (Lamontagne et al.,  
231 2001), is used in this study.

232 It must be noted here that the carbonyl group is typically defined in the range of  
233  $1655\text{-}1760\text{ cm}^{-1}$ , representing mostly the formation of ketones (Lamontagne et al., 2001;

234 Petersen & Glaser, 2011). However, the rejuvenator used shows a peak around 1740  
 235  $\text{cm}^{-1}$ , corresponding to carbonyl esters, which hinders the accurate integration of the  
 236 carbonyl area. To avoid possible overestimation of the carbonyl index due to the  
 237 rejuvenator presence, the baseline limit of the carbonyl group was set between 1655 and  
 238  $1720 \text{ cm}^{-1}$ . All the considered indices and their limits are presented in Table 2.

239 Table 2: Functional groups, baseline limits and their corresponding indices

Functional group	Baseline limits ( $\text{cm}^{-1}$ )	Index
Aliphatic group ( $A_{\text{ref}}$ )	1350-1395 + 1395-1515	
Carbonyl group ( $A_{\text{CO}}$ )	1655-1720	$I_{\text{CO}} = A_{\text{CO}}/A_{\text{ref}}$
Sulfoxide group ( $A_{\text{SO}}$ )	986-1047	$I_{\text{SO}} = A_{\text{SO}}/A_{\text{ref}}$
Polybutadiene group ( $A_{\text{PB}}$ )	960-970	$I_{\text{PB}} = A_{\text{PB}}/A_{\text{ref}}$
Polystyrene group ( $A_{\text{PS}}$ )	695-705	$I_{\text{PS}} = A_{\text{PS}}/A_{\text{ref}}$

240 Since compatibility between the different components of the blends is crucial,  
 241 microscopic images were captured using fluorescence microscopy to observe the  
 242 morphology of binder blends. The microscope is a Carl Zeiss Axioskop 40Fl with an  
 243 HBO 50 light source, while a deltapix DP200 digital camera is used to capture the  
 244 images. Different protocols have been suggested to investigate PMB using fluorescence  
 245 **microscopy (Kou et al., 2019)**. The thin-film method is selected for sample preparation  
 246 in this study to investigate storage stability. First, the binder blends were homogenised,  
 247 and then a hot drop of the blend was placed between two glass plates, resulting in a thin  
 248 layer of bitumen. Next, the sample was isothermally stored for 30 minutes at  $160^{\circ}\text{C}$ .  
 249 Then, the samples were immediately inspected with the microscope. Due to the thin  
 250 sample size, the sample cooled down rather quickly during the test.

## 251 **Results and discussion**

### 252 *Conventional tests*

253 The results of the conventional tests are presented in Table 3. The effect of the polymer  
 254 modification in the reference PMB can be clearly observed by the high softening point

255 and PI. The 100% RPMB sample seemed heavily aged, with a penetration value of  
 256 10 x 0.1 mm. Due to the relatively moderate softening point of this binder, the PI is  
 257 negative, which indicates that the residual effect of polymer modification is relatively  
 258 small. Note that a negative PI can also be interpreted as a sign of non-modified binder.  
 259 Thus, RPMB exhibited signs of severe polymer degradation.

260 **Table 3: Penetration, softening point and penetration index of the blends**

		20%	40%	60%	20%	40%	60%	100%
	REF	REJ	REJ	REJ	RA	RA	RA	RA
Penetration (0.1mm)	51	52	52	53	46	28	25	10
Softening point (°C)	76.4	69.8	52.6	53.6	70.4	61.0	63.2	68.6
Penetration index	3.84	2.89	-0.46	-0.20	2.65	-0.06	0.08	-0.48

261 As expected, the non-rejuvenated blends (20% RA, 40% RA and 60% RA)  
 262 showed a decrease in penetration value with increasing RA content. However, the  
 263 evolution of the softening point is less obvious. Above 20% RA, there is a remarkable  
 264 drop in softening point below the values of the two constituent binders. This  
 265 phenomenon might be caused by the dilution of the polymer content in the blend due to  
 266 the high RA binder content, which appeared to contain inactive polymers. At a  
 267 recycling rate of 60%, the softening point slightly increased again because of the higher  
 268 percentage of aged binder. Due to the relationship between softening point and PI, the  
 269 same trend was observed in PI values.

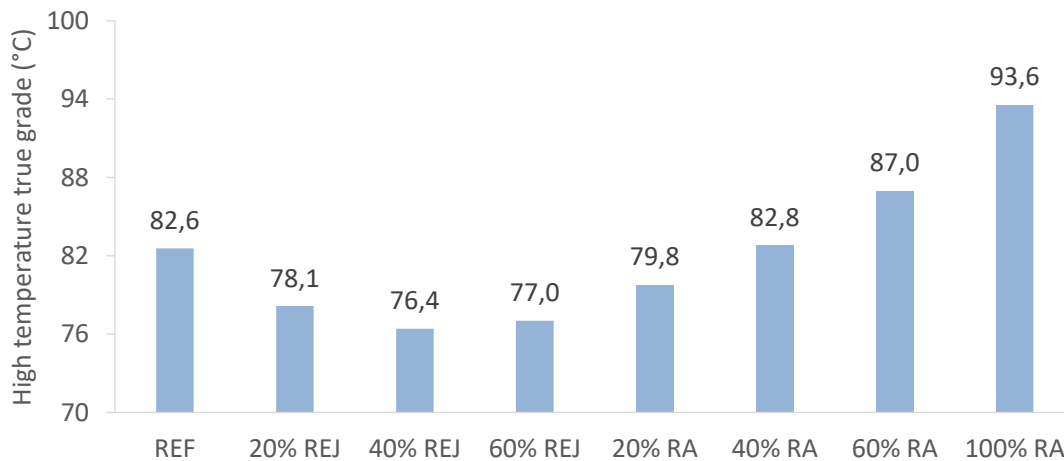
270 The penetration values of the rejuvenated blends were similar to that of the  
 271 reference binder, as intended in the experiment design. The softening point followed a  
 272 similar trend as their non-rejuvenated counterparts: a relatively high value for the 20%  
 273 recycling rate, the lowest value at 40%, and a slight increase for the 60% recycling rate.  
 274 Due to the softening effect of the rejuvenator, the softening points at high recycling  
 275 rates dropped significantly compared to the non-rejuvenated blends.

276 ***Rheological characterisation***

277 *High-temperature true grade*

278 The high-temperature true grade is used to investigate the performance of the blends at  
279 temperatures where the polymer is more likely to be active. The high-temperature true  
280 grade of the non-rejuvenated blends increased alongside the increase in recycling rate,  
281 as shown in Figure 2. The increasing trend substantiates the stiffening effect of adding  
282 RA, which was also observed from conventional properties. Conversely, the addition of  
283 rejuvenator caused a softening effect, leading to lower true grade values. All  
284 rejuvenated blends yielded similar values, which agrees with the trend observed in  
285 binder penetration.

286 The softening point and the high-temperature true grade show a different trend.  
287 The softening point seemed to be more susceptible to the presence of virgin polymer,  
288 whereas the true grade was mainly driven by binder hardening.



289

290 **Figure 2: Bar chart of the high-temperature true grade of blends**

291 *Master curve*

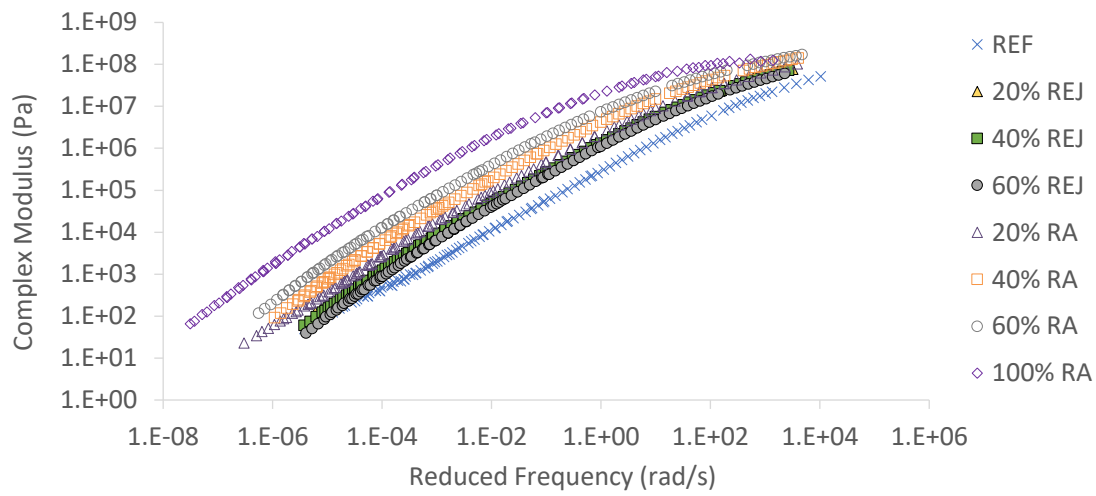
292 **Figure 3 and Figure 4 show the master curve averages for complex modulus and phase**  
293 **angle, respectively. All measurements were within the precision described in EN**

294 14770:2012, namely below 10% and 5% for  $G^*$  and delta, respectively. The  
295 root-mean-square error of the fitted CA models ranged between 3.64% and 6.95%, and  
296 the  $R^2$  was above 98.9% for all binder blends.

297 Complex modulus results ranged from the lowest values, exhibited by the  
298 reference binder, to the highest values exhibited by the recovered RPMB. The addition  
299 of RPMB increased the complex modulus of the blends without rejuvenator at all  
300 frequencies. However, the three blends with rejuvenator exhibited a similar complex  
301 modulus throughout the range of frequencies despite the different recycling content.  
302 This means that the rejuvenator content determined to target the same penetration value  
303 yielded blends of similar stiffness over the entire frequency range.

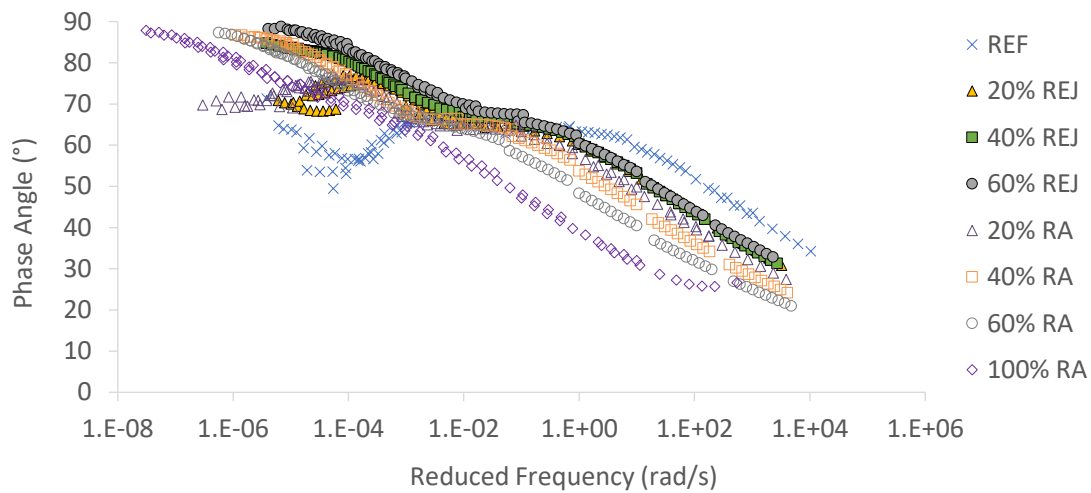
304 As illustrated in Figure 4, the reference binder displayed multiple phase angle  
305 values around 1.E-05 rad/s most likely due to segregation of the polymer. This  
306 segregation can be the result of non-isothermal cooling or slow heating, as concluded by  
307 Soenen et al. (Soenen et al., 2008). Note also that the reference binder exhibited a  
308 plateau between 1 rad/s and 1.E-03 rad/s, and even a slight decrease in phase angle at  
309 frequencies below 1.E-03 rad/s (equivalent to the response at high temperatures), as  
310 expected from the more elastic response of PMB. This effect known in the literature as  
311 'feathering' occurs when a polymer is present and active (Mensching et al., 2016).  
312 Similarly, blends with 20% RAB (with and without rejuvenator) showed an attempt to  
313 maintain the phase angle at lower frequencies, which indicates a certain level of  
314 polymer activity. Conversely, blends with 40% RAB and above showed a continuous  
315 decrease in phase angle with increasing frequency, which is characteristic of binders  
316 with no polymer or negligible polymer response. For frequencies above 0.1 rad/s, all  
317 blends with rejuvenators yielded almost the same phase angle, which was higher than  
318 that of blends without rejuvenator, indicating the presence of a rejuvenator increased the

319 viscous response and higher frequencies. This may be indicative of a better ability to  
320 relax stresses at lower temperatures.



321

322 Figure 3: Complex modulus master curves of the binders



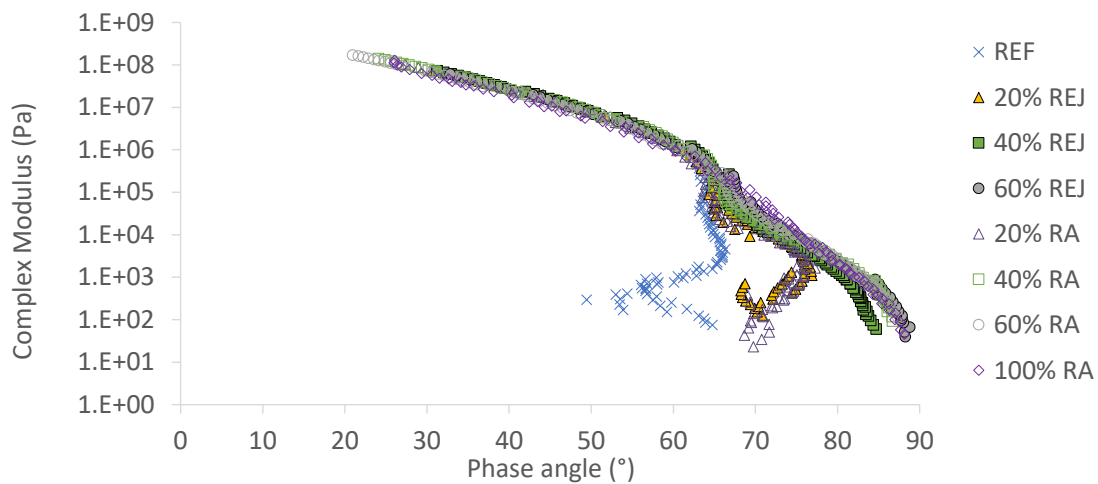
323

324 Figure 4: Phase angle master curves of the binders

325 *Black curve*

326 Figure 5 illustrates the black curve of the eight binders in complex modulus-phase angle  
327 space. All binders exhibited a similar response for complex modulus above  $1E+05$  Pa,  
328 which corresponds to the intermediate- and low-temperature range. Below  $1E+05$  Pa,  
329 the reference binder showed a relatively constant phase angle, followed by a reduction

330 and a slight increase. This characteristic response of PMB binders, known as ‘curling’,  
 331 substantiated the presence of polymer in the virgin PMB. The two blends with 20%  
 332 RPMB, which yielded a plateau in phase angle at low reduced frequencies, also showed  
 333 signs of polymer activity. Out of the remaining binder samples, only that with 40%  
 334 RPMB and rejuvenator exhibited a minimal sign of polymer response. Based on black  
 335 curve results, the addition of the rejuvenator did not noticeably restore the elasticity of  
 336 the blends with RPMB. The 100% RA sample does not show any remaining polymer  
 337 activity, which agrees with a previous study on field aged binders (Margaritis et al.,  
 338 2020).



339

340 Figure 5: Black diagram of the binder blends.

341 *Multiple stress creep-recovery test*

342 Table 4 confirms the findings from phase angle and black curve: the reference binder  
 343 and both blends with 20% RPMB exhibited low non-recoverable compliance and high  
 344 strain recovery (above 90%), which is characteristic of polymer activity. Above 20%  
 345 RPMB, the blends experienced a 50% drop in strain recovery and, potentially, greater  
 346 susceptibility to permanent deformation at higher temperatures. The softening effect of  
 347 the rejuvenator tended to make the blends more compliant and less elastic (lower strain

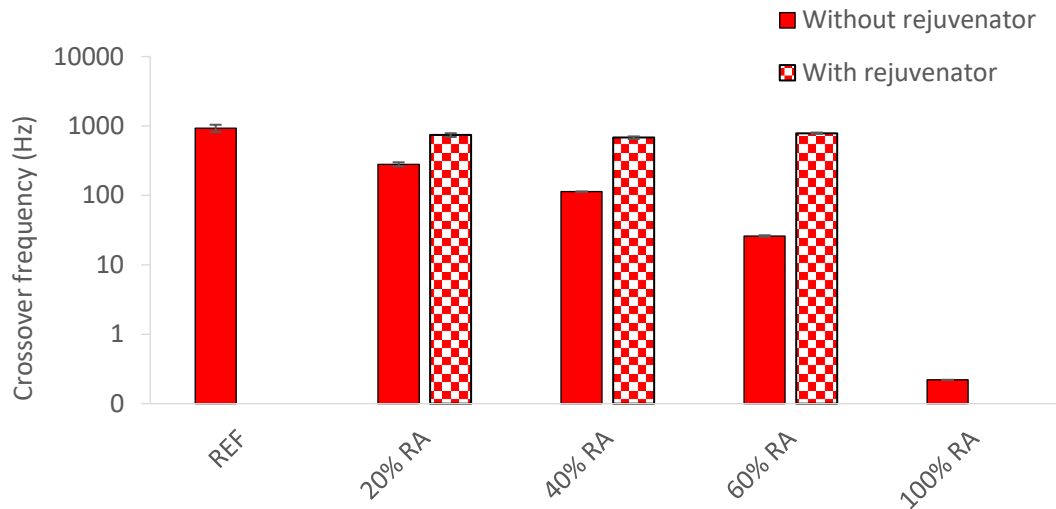
348 recovery), particularly at 60% RPMB.

349 **Table 4: Penetration, softening point and penetration index of the blends**

	20%	40%	60%	20%	40%	60%	100%
	REF	REJ	REJ	REJ	RA	RA	RA
$J_{nr,100Pa}$ (kPa <sup>-1</sup> )	0.02	0.05	0.27	0.50	0.05	0.11	0.06
$J_{nr,3200 Pa}$ (kPa <sup>-1</sup> )	0.01	0.02	0.26	0.56	0.02	0.11	0.06
$R_{100}$ (Pa)	93.4%	92.5%	53.1%	24.6%	91.9%	44.2%	45.0%
$R_{3200}$ (Pa)	96.2%	94.2%	49.7%	14.3%	94.3%	40.4%	43.8%

350 *Crossover frequency*

351 The crossover frequency is given in Figure 6 for the different recycling rates, with and  
352 without rejuvenator. The non-rejuvenated blends show a gradual, almost linear decrease  
353 with increasing RPMB content, which can be interpreted as a decline in the viscous  
354 component. A reduction in the viscous component reduces the ability to relax stresses,  
355 which may increase the susceptibility to low-temperature cracking (D. W. Christensen  
356 et al., 2017; Jing et al., 2020; G. M. Rowe & Sharrock, 2016). Conversely, the crossover  
357 frequency remained relatively constant for the rejuvenated blends. This means the  
358 rejuvenator compensated for the stiffening effect of increasing recycling rate and kept  
359 the balance between the elastic and viscous components. As a result, the addition of the  
360 rejuvenator seems to have a positive effect on the ability to relax stresses at low  
361 temperatures. The results of this study are in line with previous investigations on non-  
362 modified RAB blends. Previous studies indicated that both ageing and an increase in  
363 recycling rate decreased the crossover frequency (Gómez-Meijide et al., 2018), whereas  
364 the opposite effect happened with the addition of rejuvenators (Dhasmana et al., 2019).



365

366 **Figure 6: Evolution of crossover frequency with increasing recycling rate, with and**  
 367 **without rejuvenator.**

368 *Glover-Rowe parameter*

369 G-R values and damage thresholds are depicted in a black space diagram in Figure 7.

370 All blends fell in the no damage region apart from the 100% RA; the level of field

371 ageing experienced by this binder made it prone to damage. For the non-rejuvenated

372 blends, the G-R parameter shifted up to the left. This observation confirms that both

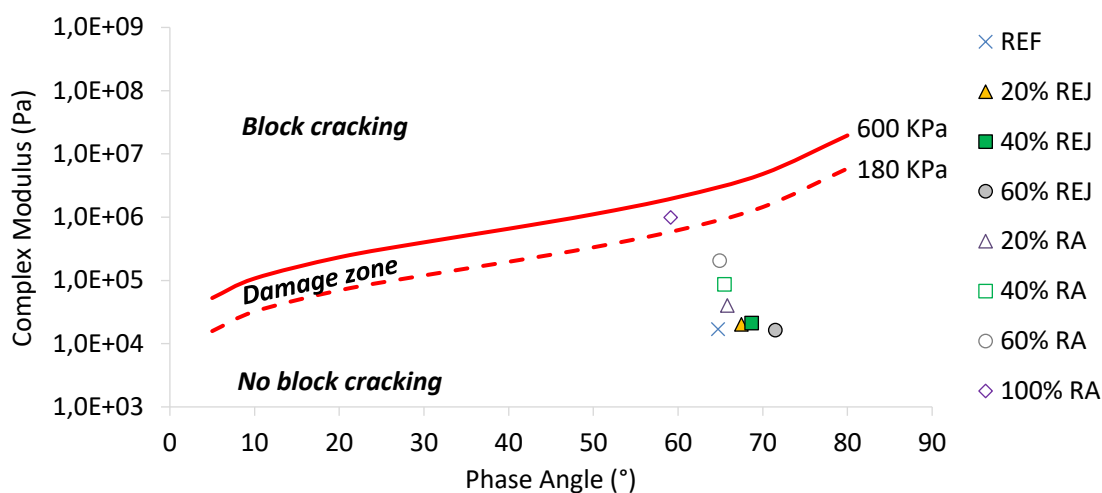
373 ageing and increasing recycling rate result in a higher susceptibility to cracking.

374 Furthermore, all rejuvenated blends provided G-R values similar to that of of the

375 reference binder, with the difference being a slight increase in phase angle with

376 increasing RPMB content. Both G-R and crossover frequency results proved that the

377 addition of this rejuvenator was beneficial in terms of non-load-associated cracking.



378

379 Figure 7: Glover-Rowe parameters plotted with the limit thresholds in a black space  
 380 diagram

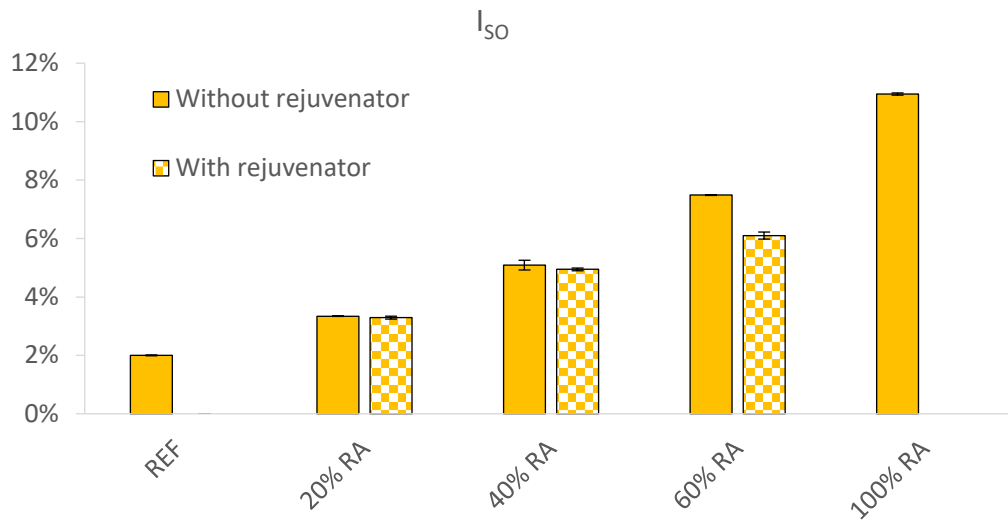
### 381 **Physicochemical characterisation**

#### 382 *FTIR spectroscopy*

383 The sulfoxide and carbonyl indices were calculated to examine ageing level, whereas  
 384 the polybutadiene and polystyrene indices were used as polymer-related indices. The  
 385 calculated sulfoxide indices are presented in Figure 8. This study found an increasing  
 386 trend in sulfoxide indices with increasing recycling rate. As depicted in Figure 8 the  
 387 increase in recycling rate resulted in an almost linear increase for both blends, with and  
 388 without rejuvenator.

389 The inclusion of rejuvenator at lower recycling rates (20% and 40%) did not  
 390 have a substantial effect. On the other hand, a decrease in the sulfoxide index is  
 391 observed for the 60% RPMB sample. In fact, an increase in polarity is accompanied by  
 392 the formation of sulfoxide-related moieties, possibly present in the more polar fractions  
 393 such as asphaltenes. The addition of rejuvenator is expected to increase the maltene  
 394 fraction and, consequently, to proportionally reduce the asphaltene component. The  
 395 expected increase in total sulfoxide groups associated with ageing can be visualised in

396 Figure 8 as a result of the further addition of aged RPMB. Consequently, the reduction  
 397 in the sulfoxide index is linked to the increasing dosage of rejuvenator, especially  
 398 noticeable on the 60% RA blend (Figure 8). From these results, it can be assumed that  
 399 the use of rejuvenator, especially at a higher dosage, can be regarded as beneficial in  
 400 terms of ageing, especially at higher recycling rates.

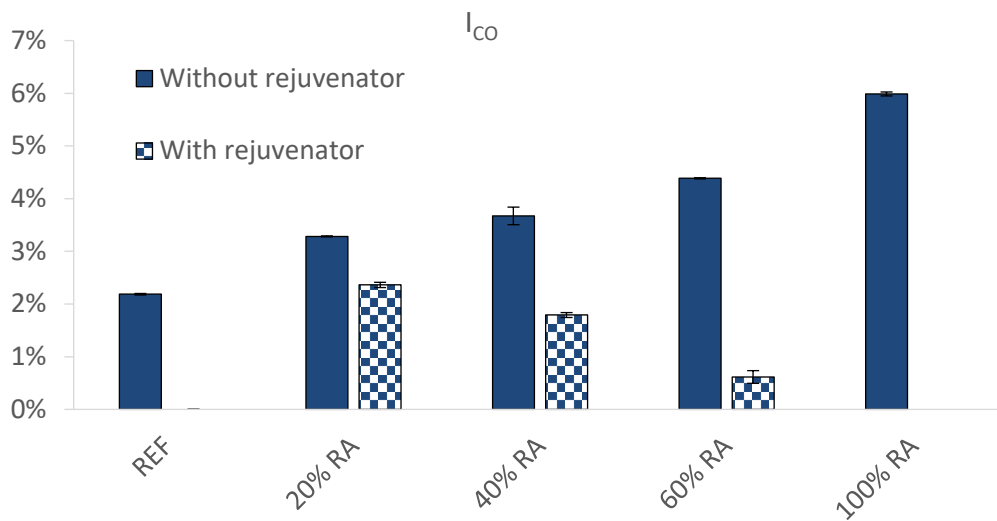


401

402 Figure 8: Evolution of sulfoxide index with increasing recycling rate and with  
 403 rejuvenator presence.

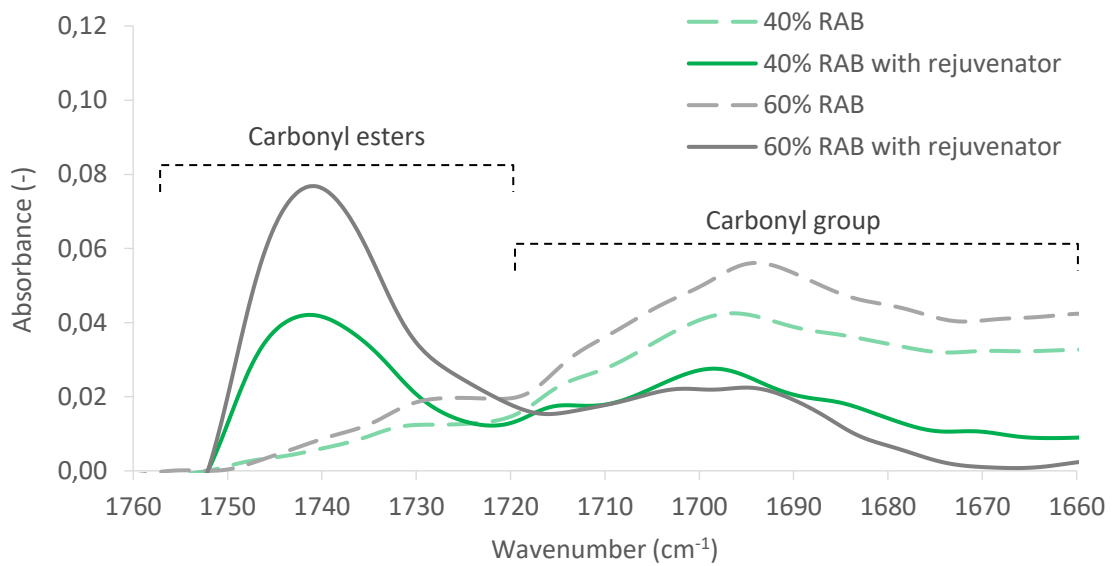
404 Similarly to the sulfoxide index, the carbonyl index (depicted in Figure 9)  
 405 increased almost linearly with the increase in recycling rate, an observation now only  
 406 valid for the non-rejuvenated samples. Conversely, the inclusion of rejuvenator led to a  
 407 decrease in the carbonyl index. A more in-depth inspection of the actual spectra, given  
 408 in Figure 10, revealed an overlap between the peaks of the carbonyl esters group  
 409 ( $1700-1760\text{ cm}^{-1}$ ) corresponding to the rejuvenator, and the carbonyl group ( $1655-1760$   
 410  $\text{cm}^{-1}$ ) coming from the aged binder, an issue already discussed in the methods section.  
 411 The rise in rejuvenator dosage led to a decrease in the absolute absorbance value around  
 412  $1700\text{ cm}^{-1}$ , and that may indicate a partial restoration effect. However, considering the  
 413 area integration, part of the carbonyl group is not encountered when considering a

414 narrower band (1655-1720 instead of 1655-1760  $\text{cm}^{-1}$ ), which led to an underestimation  
 415 of the carbonyl index. However, consideration of a wider band would have led to an  
 416 overestimation of the carbonyl index due to carbonyl ester peak. Consequently, it can be  
 417 concluded that the assessment of the carbonyl index in blends with rejuvenator is  
 418 considered problematic.



419

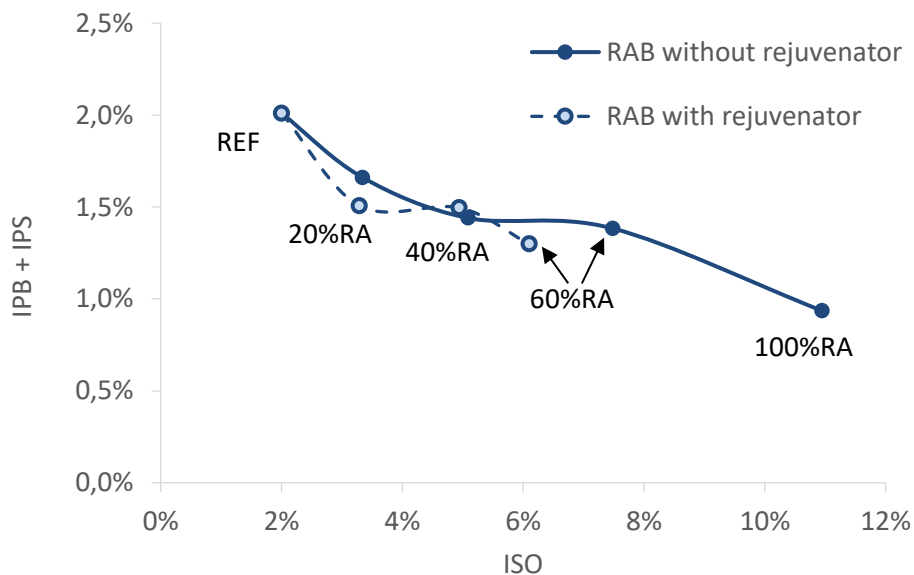
420 Figure 9: Evolution of carbonyl index with increasing recycling rate and with  
 421 rejuvenator presence.



422

423 Figure 10: FTIR spectra of the overlapping peaks of carbonyl and rejuvenator

424 For a critical assessment of the degradation level of the SBS polymer, the two  
 425 indices responsible for this phenomenon ( $I_{PS}$  and  $I_{PB}$ ) were utilised. Since the ultimate  
 426 goal was to reflect the degradation level of the polymer, a cumulative polymer index,  
 427 i.e. the sum of polystyrene ( $I_{PS}$ ) and polybutadiene ( $I_{PB}$ ), was employed here. From the  
 428 previous FTIR analysis, it becomes apparent that the carbonyl index will not depict the  
 429 actual ageing severity accurately when rejuvenators, like the one considered in this  
 430 study, are included in the blend. For that reason, the sulfoxide index ( $I_{SO}$ ) is regarded as  
 431 the most appropriate value to evaluate ageing severity, from a chemical perspective, for  
 432 all the blends in this study. A comparative plot of the cumulative polymer index and the  
 433  $I_{SO}$  allows for a quantification of polymer degradation (Figure 11).



434

435 Figure 11: Cumulative polymer index versus ageing index for different recycling rates

436 The overall trend is a simultaneous decrease in the cumulative polymer index  
 437 and the sulfoxide index with increasing recycling rate. The reduction in cumulative  
 438 polymer index indicates scission of polymer chains. It can be concluded that the  
 439 inclusion of RPMB has a similar effect as bitumen ageing. In terms of polymer  
 440 restoration, the rejuvenator appears to not improve the RPMB at 20% recycling rate

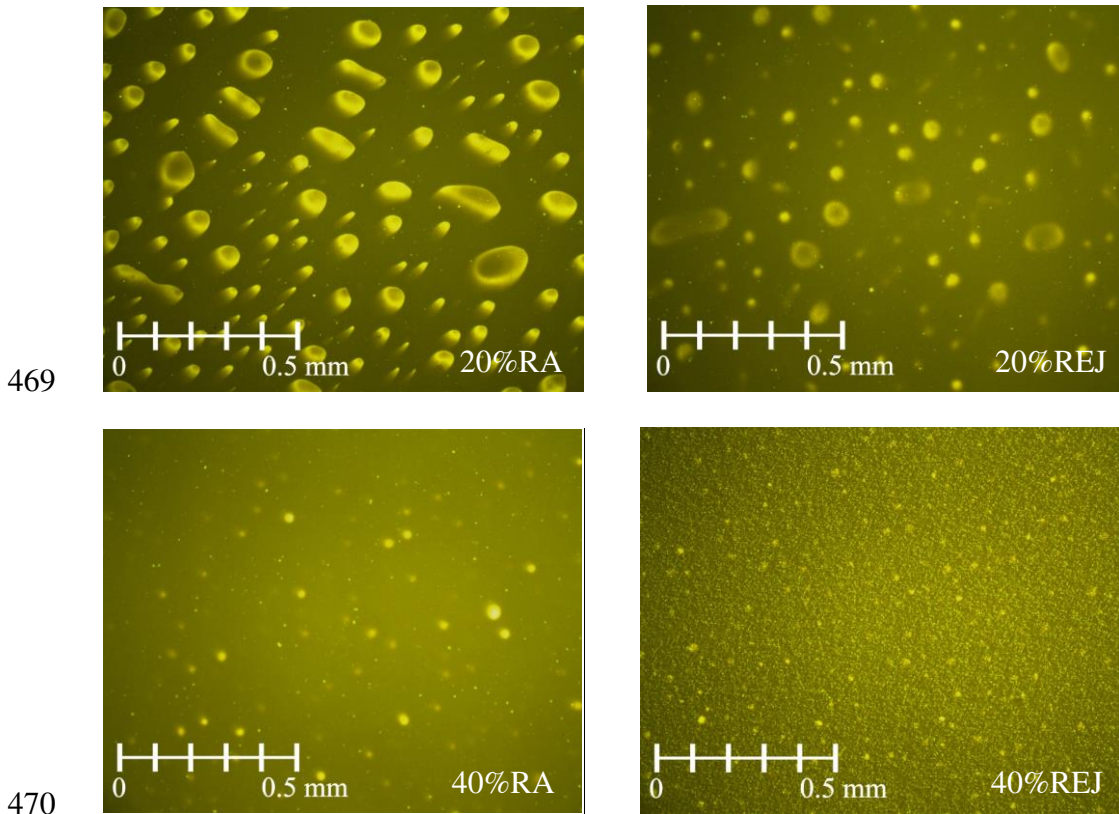
441 compared to the same non-rejuvenated blend, while similar ageing severity is observed  
442 for this recycling rate. This finding might be an indication that the rejuvenator has an  
443 adverse effect on the compatibility of the virgin PMB with the RPMB. Conversely, the  
444 addition of rejuvenator appeared to be beneficial up to 40%, as indicated by the plateau  
445 in Figure 11 (polymer degradation remained somehow stable). More specifically, these  
446 plateaus seem to range between 20 and 40% RA when adding rejuvenator and between  
447 40 and 60% RA without rejuvenator. For 40% and 60% RA, the rejuvenator appears to  
448 have little effect on polymer restoration compared to the blends without rejuvenator.  
449 Among the evaluated blends with and without rejuvenator, polymer degradation is most  
450 evident for a recycling rate of 60%.

#### 451 *Fluorescence microscopy*

452 It is also critical to assess the impact of the recycling rate and rejuvenator on bitumen  
453 morphology. The findings from the FTIR analysis indicated that rejuvenated blends  
454 with 20% and 40% RPMB exhibited a similar level of polymer degradation despite the  
455 increased aged RPMB content of the latter. Thus, the focus of the microscopic  
456 investigation is exclusively on these two recycling rates to better understand the  
457 influence that the rejuvenator may have on the polymer phase. The microscopic images  
458 are depicted in **Figure 12**. It appeared that the increase in RPMB content led to a  
459 shrinkage and a total reduction in the polymer-rich phase for blends with and without  
460 rejuvenator (**Figure 12**).

461 The impact of the rejuvenator on blend morphology is depicted on the right side  
462 of **Figure 12**. For 20% RPMB, the number and size of polymer particles was found to  
463 decrease, which may have an association with the compatibility between the  
464 compounds. For 40% RPMB, the number of round polymer particles seemed to increase

465 for the rejuvenated blend, although their size appears smaller. The reason for these  
466 changes in bitumen morphology is still an open question that requires further  
467 investigation on SBS compatibility in the new blend as well as on the compatibility of  
468 the rejuvenator in the blends.



471 **Figure 12: Fluorescence images (x100) of selected recycling rates and the effect of**  
472 **rejuvenator**

### 473 **Conclusions and recommendations**

474 A chemo-rheological investigation was performed on blends of virgin PMB with 0%,  
475 20%, 40%, 60% and 100% of reclaimed PMB (RPMB), recovered from an actual  
476 surface layer mixture. Additionally, rejuvenated blends were produced for the 20%,  
477 40% and 60% recycling rates by adding a bio-based, tall oil rejuvenator. The following  
478 findings were made:

- 479
- Even though the presence of SBS polymer in RPMB was verified with FTIR, all

480 tests showed severe polymer degradation and no signs of residual polymer  
481 activity in the recovered binder, especially noticeable for the 60% and 100%  
482 recycling rates. Furthermore, the recovered binder exhibited high susceptibility  
483 to non-load-associated cracking according to the Glover-Rowe parameter. This  
484 is a key finding for recycling aged PMB in new asphalt mixtures.

485 • Polymer dilution lowered the softening point at recycling rates of 20% and 40%  
486 whereas an increase in softening point was observed at 60% due to the high  
487 content of hard, aged binder. The softening point seemed to be more susceptible  
488 to the presence of virgin polymer, whereas the high-temperature true grade was  
489 mainly driven by binder hardening.

490 • Using a fixed target penetration to dose the rejuvenator led to blends with  
491 similar high-temperature true grade and master curves. This is not necessarily  
492 intuitive since binder penetration is measured at 25°C, high-temperature true  
493 grade is defined by a fixed stiffness and phase angle, and master curves are  
494 obtained over a range of temperatures and frequencies.

495 • The carbonyl index, frequently used as an indication of binder ageing level, may  
496 be influenced by the presence of carbonyl esters in the rejuvenator. Therefore,  
497 the use of a carbonyl index that accounts only for the carbonyl present, by  
498 considering a narrower wavelength range between 1655-1720  $\text{cm}^{-1}$ , is highly  
499 recommended.

500 The following conclusions can be drawn from the results of this investigation:

501 • In addition to the known stiffening effect, the addition of RPMB increased the  
502 susceptibility of the blends to non-load-associated cracking as evidenced by the  
503 crossover frequency and Glover-Rowe parameter. Furthermore, fluorescence

504 microscopy revealed that adding RPMB reduced the polymer-rich phase of the  
505 blends due to the lack of activity of the polymer present in RPMB.

506 • The rejuvenator used in this study did not activate or increase the level of  
507 activity of the aged polymer present in RPMB. However, this rejuvenator  
508 successfully compensated for the stiffening effect of the aged binder and  
509 reduced the susceptibility to non-load-associated cracking to levels comparable  
510 to those of the virgin PMB binder.

511 • Several rheological test results (phase angle master curve, black curve, and  
512 MSCR) confirmed the characteristic ‘feathering’ and ‘curling’ effects associated  
513 with active polymer presence on blends up to 20% RPMB for the used materials.  
514 The blend with 40% RPMB and rejuvenator showed minimal polymer activity in  
515 the black curve and MSCR test. All other blends performed as non-polymer-  
516 modified binders.

517 This study describes a first attempt to recycle RPMB in new premium surface layers by  
518 investigating the effect of using an RPMB source and exploring which tests can be useful  
519 to capture the possible residual activity of the aged polymer on binder scale. Future work  
520 is necessary to further assess the potential of recycling PMB by upscaling the  
521 experimental procedure, going from a binder level to a mixture level. This will also allow  
522 to better capture the actual degree of blending instead of the full blending scenario of  
523 binder testing. Finally, additional tests such as low-temperature cracking should also be  
524 performed in a future study. This knowledge is of paramount importance to allow  
525 recycling in premium asphalt surfaces and stop downcycling high-quality RAP  
526 containing aged PMB milled from surface layers.

## 527 **Disclosure statement**

528 The authors reported no potential conflict of interest.

529 **Acknowledgements**

530 The authors would like to acknowledge Hilde Soenen from Nynas NV for her assistance  
531 on the fluorescence microscopy and her valuable comments. Also, Koen Deckers from  
532 BAM Contractors for providing the RA material.

533 **References**

- 534 Abatech. (2011). *RHEA-Rheology Analysis Software, version 2.3* (  
535 Agentschap Wegen en Verkeer. (2019). *Standaardbestek 250 voor de wegenbouw -*  
536 *versie 4.1.* (  
537 Airey, G. D. (2003). Rheological properties of styrene butadiene styrene polymer  
538 modified road bitumens. *Fuel*, 82(14), 1709-1719.  
539 [https://doi.org/https://doi.org/10.1016/S0016-2361\(03\)00146-7](https://doi.org/https://doi.org/10.1016/S0016-2361(03)00146-7)  
540 Anthonissen, J., Van den bergh, W., & Braet, J. (2016). Review and environmental  
541 impact assessment of green technologies for base courses in bituminous  
542 pavements. *Environmental Impact Assessment Review*, 60, 139-147.  
543 <https://doi.org/https://doi.org/10.1016/j.eiar.2016.04.005>  
544 Aurangzeb, Q., Al-Qadi, I. L., Ozer, H., & Yang, R. (2014). Hybrid life cycle  
545 assessment for asphalt mixtures with high RAP content. *Resources,*  
546 *Conservation and Recycling*, 83, 77-86.  
547 <https://doi.org/https://doi.org/10.1016/j.resconrec.2013.12.004>  
548 Bajaj, A., Epps Martin, A., King, G., Glover, C., Kaseer, F., & Arámbula-Mercado, E.  
549 (2020). Evaluation and classification of recycling agents for asphalt binders.  
550 *Construction and Building Materials*, 260, 119864.  
551 <https://doi.org/https://doi.org/10.1016/j.conbuildmat.2020.119864>  
552 Christensen, D., Mensching, D., Rowe, G., Anderson, R. M., Hanz, A., Reinke, G., &  
553 Anderson, D. (2019). *Past, Present, and Future of Asphalt Binder Rheological*  
554 *Parameters: Synopsis of 2017 Technical Session 307.* 96th Annual Meeting of  
555 the Transportation Research Board.  
556 Christensen, D. W., Anderson, D. A., & Rowe, G. M. (2017). Relaxation spectra of  
557 asphalt binders and the Christensen–Anderson rheological model. *Road*  
558 *Materials and Pavement Design*, 18(sup1), 382-403.  
559 <https://doi.org/10.1080/14680629.2016.1267448>  
560 Christensen, D. W. J., & Anderson, D. A. (1992). Interpretation of dynamic mechanical  
561 test data for paving grade asphalt (*Asphalt Paving Technology: Association of*  
562 *Asphalt Paving Technologists-Proceedings of the Technical Sessions.*  
563 D'Angelo, J., Kluttz, R., Dongre, R. N., Stephens, K., & Zanzotto, L. (2007). Revision  
564 of the superpave high temperature binder specification: the multiple stress creep  
565 recovery test (with discussion). *Journal of the Association of Asphalt Paving*  
566 *Technologists*, 76.  
567 Dhasmana, H., Hossain, K., & Karakas, A. S. (2019). Effect of long-term ageing on the  
568 rheological properties of rejuvenated asphalt binder. *Road Materials and*  
569 *Pavement Design*, 1-19. <https://doi.org/10.1080/14680629.2019.1686051>  
570 Domingos, M. D. I., & Faxina, A. L. (2016). Susceptibility of Asphalt Binders to  
571 Rutting: Literature Review. *Journal of Materials in Civil Engineering*, 28(2).  
572 [https://doi.org/https://doi:10.1061/\(ASCE\)MT.1943-5533.0001364](https://doi.org/https://doi:10.1061/(ASCE)MT.1943-5533.0001364)

- 573 Garcia Cucalon, L., Kaseer, F., Arámbula-Mercado, E., Epps Martin, A., Morian, N.,  
574 Pournoman, S., & Hajj, E. (2019). The crossover temperature: significance and  
575 application towards engineering balanced recycled binder blends. *Road*  
576 *Materials and Pavement Design*, 20(6), 1391-1412.  
577 <https://doi.org/https://doi.org/10.1080/14680629.2018.1447504>
- 578 Gómez-Meijide, B., Ajam, H., Lastra-González, P., & Garcia, A. (2018). Effect of  
579 ageing and RAP content on the induction healing properties of asphalt mixtures.  
580 *Construction and Building Materials*, 179, 468-476.  
581 <https://doi.org/https://doi.org/10.1016/j.conbuildmat.2018.05.121>
- 582 Hofko, B., Porot, L., Falchetto Cannone, A., Poulidakos, L., Huber, L., Lu, X.,  
583 Mollenhauer, K., & Grothe, H. (2018). FTIR spectral analysis of bituminous  
584 binders: reproducibility and impact of ageing temperature. *Materials and*  
585 *Structures*, 51(2), 45. <https://doi.org/https://doi.org/10.1617/s11527-018-1170-7>
- 586 Jacobs, G., Margaritis, A., Hernando, D., He, L., Blom, J., & Van den bergh, W. (2021).  
587 Influence of soft binder and rejuvenator on the mechanical and chemical  
588 properties of bituminous binders. *Journal of Cleaner Production*, 287.  
589 <https://doi.org/10.1016/j.jclepro.2020.125596>
- 590 Jing, R., Varveri, A., Liu, X., Scarpas, A., & Erkens, S. (2020). Rheological, fatigue and  
591 relaxation properties of aged bitumen. *International Journal of Pavement*  
592 *Engineering*, 21(8), 1024-1033. <https://doi.org/10.1080/10298436.2019.1654609>
- 593 Kleiziene, R., Panasenkiene, M., & Vaitkus, A. (2019). Effect of Aging on Chemical  
594 Composition and Rheological Properties of Neat and Modified Bitumen.  
595 *Materials (Basel)*, 12(24). <https://doi.org/10.3390/ma12244066>
- 596 Kodippily, S., Holleran, G., & Henning, T. F. P. (2017). Deformation and cracking  
597 performance of recycled asphalt paving mixes containing polymer-modified  
598 binder. *Road Materials and Pavement Design*, 18(2), 425-439.  
599 <https://doi.org/10.1080/14680629.2016.1181559>
- 600 Kou, C., Xiao, P., Kang, A., Mikhailenko, P., Baaj, H., & Wu, Z. (2019). Protocol for  
601 the morphology analysis of SBS polymer modified bitumen images obtained by  
602 using fluorescent microscopy. *International Journal of Pavement Engineering*,  
603 20(5), 585-591. <https://doi.org/10.1080/10298436.2017.1316647>
- 604 Lamontagne, J., Dumas, P., Mouillet, V., & Kister, J. (2001). Comparison by Fourier  
605 transform infrared (FTIR) spectroscopy of different ageing techniques:  
606 application to road bitumens. *Fuel*, 80(4), 483-488.  
607 [https://doi.org/https://doi.org/10.1016/S0016-2361\(00\)00121-6](https://doi.org/https://doi.org/10.1016/S0016-2361(00)00121-6)
- 608 Lesueur, D. (2009). The colloidal structure of bitumen: Consequences on the rheology  
609 and on the mechanisms of bitumen modification. *Advances in Colloid and*  
610 *Interface Science*, 145(1), 42-82.  
611 <https://doi.org/https://doi.org/10.1016/j.cis.2008.08.011>
- 612 Liu, G., Nielsen, E., Komacka, J., Leegwater, G., & van de Ven, M. (2015). Influence  
613 of soft bitumens on the chemical and rheological properties of reclaimed  
614 polymer-modified binders from the “old” surface-layer asphalt. *Construction*  
615 *and Building Materials*, 79, 129-135.  
616 <https://doi.org/https://doi.org/10.1016/j.conbuildmat.2015.01.002>
- 617 Lu, X., & Isacson, U. (1998). Chemical and rheological evaluation of ageing properties  
618 of SBS polymer modified bitumens. *Fuel*, 77(9), 961-972.  
619 [https://doi.org/https://doi.org/10.1016/S0016-2361\(97\)00283-4](https://doi.org/https://doi.org/10.1016/S0016-2361(97)00283-4)
- 620 Margaritis, A., Soenen, H., Fransen, E., Pipintakos, G., Jacobs, G., Blom, J., & Van den  
621 bergh, W. (2020). Identification of ageing state clusters of reclaimed asphalt  
622 binders using principal component analysis (PCA) and hierarchical cluster

623 analysis (HCA) based on chemo-rheological parameters. *Construction and*  
624 *Building Materials*, 244, 118276.  
625 <https://doi.org/https://doi.org/10.1016/j.conbuildmat.2020.118276>

626 Marsac, P., Piérard, N., Porot, L., Van den bergh, W., Grenfell, J., Mouillet, V., Pouget,  
627 S., Besamusca, J., Farcas, F., Gabet, T., & Hugener, M. (2014). Potential and  
628 limits of FTIR methods for reclaimed asphalt characterisation [journal article].  
629 *Materials and Structures*, 47(8), 1273-1286.  
630 <https://doi.org/https://doi.org/10.1617/s11527-014-0248-0>

631 Masson, J., Collins, P., Robertson, G., Woods, J., Margeson, J. J. E., & Fuels. (2003).  
632 Thermodynamics, phase diagrams, and stability of bitumen– polymer blends.  
633 *17(3)*, 714-724.

634 Mensching, D. J., Gibson, N. H., Andriescu, A., Rowe, G. M., & Sias, J. E. (2016).  
635 *Assessing the Applicability of Rheological Parameters to Evaluate Modified*  
636 *Binders*. International Society for Asphalt Pavements Symposium and 53rd  
637 Petersen Asphalt Research Conference, Jackson Hole, Wyoming.

638 Petersen, J. C., & Glaser, R. (2011). Asphalt Oxidation Mechanisms and the Role of  
639 Oxidation Products on Age Hardening Revisited. *Road Materials and Pavement*  
640 *Design*, 12(4), 795-819. <https://doi.org/10.1080/14680629.2011.9713895>

641 Pipintakos, G., Vincent Ching, H. Y., Soenen, H., Sjövall, P., Mühlich, U., Van  
642 Doorslaer, S., Varveri, A., Van den bergh, W., & Lu, X. (2020). Experimental  
643 investigation of the oxidative ageing mechanisms in bitumen. *Construction and*  
644 *Building Materials*, 260, 119702.  
645 <https://doi.org/https://doi.org/10.1016/j.conbuildmat.2020.119702>

646 Rowe, G., King, G., & Anderson, M. (2014). The Influence of Binder Rheology on the  
647 Cracking of Asphalt Mixes in Airport and Highway Projects. *Journal of Testing*  
648 *and Evaluation*, 42(5), 1063-1072.  
649 <https://doi.org/https://doi.org/10.1520/JTE20130245>

650 Rowe, G. M., & Sharrock, M. J. (2016). Cracking of asphalt pavements and the  
651 development of specifications with rheological measurements. (Ed.),^(Eds.). 6th  
652 Eurasphalt & Eurobitume Congress, Prague, Czech Republic.

653 Soenen, H., Lu, X., & Redelius, P. (2008). The Morphology of Bitumen-SBS Blends by  
654 UV Microscopy. *Road Materials and Pavement Design*, 9(1), 97-110.  
655 <https://doi.org/https://doi.org/10.1080/14680629.2008.9690109>

656 Yan, C., Huang, W., Xiao, F., Wang, L., & Li, Y. (2018). Proposing a new infrared  
657 index quantifying the aging extent of SBS-modified asphalt. *Road Materials and*  
658 *Pavement Design*, 19(6), 1406-1421.  
659 <https://doi.org/https://doi.org/10.1080/14680629.2017.1318082>

660 Yan, Y., Roque, R., Cocconcelli, C., Bekoe, M., & Lopp, G. (2017). Evaluation of  
661 cracking performance for polymer-modified asphalt mixtures with high RAP  
662 content. *Road Materials and Pavement Design*, 18(sup1), 450-470.  
663 <https://doi.org/https://doi.org/10.1080/14680629.2016.1266774>

664 Yan, Y., Roque, R., Hernando, D., & Chun, S. (2019). Cracking performance  
665 characterisation of asphalt mixtures containing reclaimed asphalt pavement with  
666 hybrid binder. *Road Materials and Pavement Design*, 20(2), 347-366.  
667 <https://doi.org/https://doi.org/10.1080/14680629.2017.1393002>

668 Yildirim, Y. (2007). Polymer modified asphalt binders. *Construction and Building*  
669 *Materials*, 21(1), 66-72.  
670 <https://doi.org/https://doi.org/10.1016/j.conbuildmat.2005.07.007>

671 Yut, I., & Zofka, A. (2011). Attenuated Total Reflection (ATR) Fourier Transform  
672 Infrared (FT-IR) Spectroscopy of Oxidized Polymer-Modified Bitumens.

673            *Applied Spectroscopy*, 65(7), 765-770. [https://doi.org/https://doi.org/10.1366/10-](https://doi.org/https://doi.org/10.1366/10-06217)  
674            [06217](https://doi.org/https://doi.org/10.1366/10-06217)  
675            Zaumanis, M., & Mallick, R. B. (2015). Review of very high-content reclaimed asphalt  
676            use in plant-produced pavements: state of the art. *International Journal of*  
677            *Pavement Engineering*, 16(1), 39-55.  
678            <https://doi.org/https://doi.org/10.1080/10298436.2014.893331>  
679